Pergamon

Int. J. Mech. Sci. Vol. 40, Nos. 2–3, pp. 227–235, 1998

0020–7403/98 $19.00 + 0.00

PII: S0020–7403(97)00051–9

CALCULATION OF MECHANICAL BEHAVIORS OF SHAPE MEMORY ALLOY UNDER MULTI-AXIAL LOADING CONDITIONS

M. TOKUDA*, M. YE*, M. TAKAKURA* and P. SITTNER†

* Department of Mechanical Engineering, Mie University, 1515 Kamihama, Tsu, Mie 514 Japan; and † Institute of Physics, Czech Academy of Sciences, Na Slovance 2, Prague 8, Czech Republic

Abstract—In this paper, for the calculation of the deformation behaviors of shape-memory alloy under multi-axial loading conditions with temperature changes, a two-dimensional mechanical model of polycrystalline shape memory alloy is constructed on the bases of the crystal plasticity and the deformation mechanism of shape memory alloy. In such a model, the orientation of crystal grain in the polycrystal and the loading direction can be considered. The deformation behaviors under some complex loading conditions are calculated with the model, and the results show that they are in good qualitative agreement with the experimental results.
© 1997 Published by Elsevier Science Ltd.

Keywords: shape memory alloy, multi-axial loading, modelling, constitutive equations, smart materials.

NOTATION

E_{ij} macroscopic strain
H hardening coefficient
$\mathbf{n}^{(k)}$ twinning plane normal vector for the kth transformation system
$\mathbf{m}^{(k)}$ shear direction unit vector for the kth transformation system
T temperature
T^{MS} martensite transformation starting temperature
T^{MF} martensite transformation finishing temperature
T^{AS} austenite transformation starting temperature
T^{AF} austenite transformation finishing temperature
$\alpha_{ij}^{(k)}$ the generalized Schmid factor
β temperature coefficient
γ^t transformation strain
$\gamma_{(k)}^t$ transformation strain on the kth transformation system
γ_{MAX}^t maximum transformation strain determined by its crystallographic structure
$\xi_{(k)}$ volume fraction of the kth variant martensitic phase
ε_{ij} total strain of crystal grain
ε_{ij}^t transformation strain of crystal grain
ε_{ij}^e elastic strain of crystal grain
σ_{ij} stress of crystal grain
$\tau^{(k)}$ stress on the kth transformation system
τ^M martensite transformation stress
τ^A austenite transformation stress
$\tau^{MS}(T)$ martensite transformation starting stress under temperature T
$\tau^{AF}(T)$ austenite transformation finishing stress under temperature T
τ_0^{MS} martensite transformation starting stress under reference temperature T_0
τ_0^{AF} austenite transformation finishing stress under reference temperature T_0
Σ_{ij} macroscopic stress

1. INTRODUCTION

Shape memory alloys (SMA) are at present frequently used as one of the basic elements of intelligent structures and often cited as a typical example of smart material with sensing, controlling, and actuating functions. Such excellent functions come from the unique thermo-mechanical behaviors of SMA which are resulted from the internally twinned martensite phase transformation and its reverse transformation induced by temperature and stress. The thermo-mechanical behaviors have been thoroughly studied under uniaxial loading conditions. Thus, the present industrial applications of SMA are based on uniaxial behaviors and limited to rather simple motion of actuators. In order to

use the SMA as actuators which behave three-dimensionally, we have investigated the behaviors of SMA under multi-axial loading conditions, and found that the deformation behaviors are complex, especially under the temperature change conditions [1–3]. Obviously, if we can correctly calculate the deformation behaviors in the complex loading process by a mechanical model, it would be very convenient for the design of the intelligent SMA structures.

In the recent decades, several models were proposed to describe the thermo-mechanical behaviors of SMA [4–8]. But nearly all of them are based on thermodynamics and kinetics, and only the deformation behaviors under uniaxial loading conditions are considered. Almost all the SMA in practical applications are polycrystal. Every grain in the polycrystalline medium has its own orientation, and each grain component has potentially 24 variants determined by the crystallographic structure of material, for example, in the case of Cu-base SMA. And the stress is a symmetric second-rank tensor whose number of independent variables is six though the temperature is a scalar parameter (single variable). According to the loading conditions (magnitude and direction) only in such potential variants which are in the preferential directions in the grains of the polycrystal, the transformation will be induced. That is, the stress state, and deformation or phase transformation state may be different with each other for the grains even if the polycrystalline is subjected to a simple loading, e.g., uniaxial tension. In order to include such phenomena and more importantly, to predict the thermomechanical behaviors under complex multi-axial loading conditions, based on crystal plasticity and the transformation mechanism of shape memory alloys under thermal and mechanical loading conditions, the micro-mechanics model is set up in this paper. For the comparison, some experimental results of the SMA under multi-axial loading conditions by using the thin-walled tubular specimens made of CuAlZnMn polycrystalline SMA are also summarized.

2. DEFORMATION MECHANISM OF SMA AND ITS MODELLING

2.1. *Mechanical model for phase transformation in the SMA*

Figure 1 shows schematically that the austenite structure of SMA in Fig. 1 (o) can be converted into the internally twinned martensite structure by cooling or supplying a shear stress. The process (o) → (a) shows the transformation induced by the cooling, where any significant deformation cannot be observed, and (a) → (o) shows the reverse transformation (austenite transformation) by the subsequent heating. This is the typical phenomenon of temperature-induced reversible martensite transformation in SMA.

The process (o) → (b) shows the martensite transformation induced by the shear stress τ, where a significant deformation is observed for the uniformly oriented twinned deformation, and is an important feature of stress-induced martensite transformation in SMA. Here, if the experimental temperature is above the austenite transformation finishing temperature T^{AF}, the deformation will be restored with the disappearance of the martensite after unloading (b) → (o). The relation between stress and strain in this process is shown in Fig. 1(f). This is so-called pseudoelastic behavior of SMA. But if the experimental temperature is below the austenite transformation initiating temperature T^{AS}, the reverse transformation (austenite transformation) will not take place after unloading and the deformation will be kept [(b) → (c)] as the so-called residual strain. In the following heating process (c) → (o), the residual strain will disappear, and the original state is restored for the reverse transformation. The relation between stress and strain in the process (o) → (b) → (c) → (o) is shown in Fig. 1(g). Such a process of SMA is called the shape memory effect.

For the stress-induced martensite transformation, there is a critical stress τ_0^{MS}, and thus, only when the applied stress arrives the critical stress, the stress-induced martensite transformation will take place. As in Fig. 1(d), when the applied stress τ_a is not large enough to induce the transformation, the martensite can be obtained by the assistance of cooling. The role of cooling can be seen as decreasing the critical stress for the twinned deformation. Under the small shear stress, the austenite is only with small elastic deformation (d). But when the elastically deformed austenite is cooled, the uniformly oriented martensite phase transformation will be induced (d) → (e), and a significant deformation is obtained, i.e., the small applied stress can control the direction of martensite transformation. This is one of the important reasons why the possible internal stress produced in the polycrystal will have a significant effect on the macroscopic performances of SMA, even if the

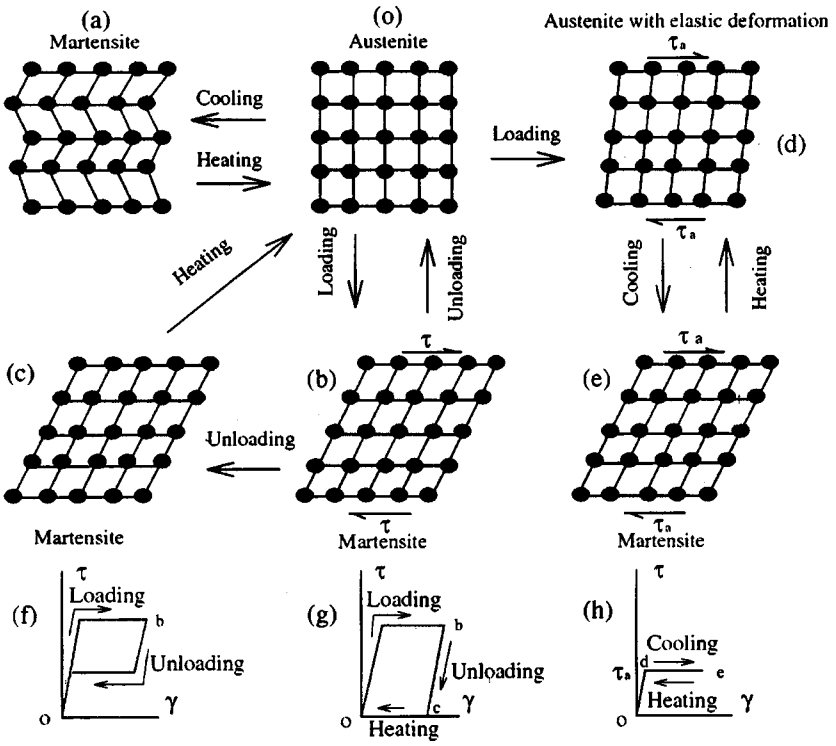

Fig. 1. Deformation mechanism of SMA.

internal stress (or residual stress) is much smaller than the critical stress. In this case the produced martensite phase and the deformation will disappear during the heating process (e) → (d). The relation between stress and strain in the process (o) → (d) → (e) → (d) is shown in Fig. 1(h). The strain will increase from (d) to (e) with the cooling, or decrease from (e) to (d) with the heating. It can be imagined that a SMA spring with such properties will expand or shrink with cooling or heating. This is the so-called two-way shape memory effect of SMA.

As seen in the above simple explanation of the deformation mechanism of the SMA, the deformation behavior or the shape-memory effect of the SMA is a combination of the temperature-induced and the stress-induced transformations between the austenite structure and the martensite structure. For example, the pseudo-elastic behavior is produced by a combination of a stress-induced martensite transformation and its reverse transformation (austenite transformation) process; the one-way shape-memory effect is the combined process of stress-induced martensite transformation and the temperature-induced reverse transformation; the two-way shape-memory effect is a process composed of temperature-induced twin transformation and its reverse transformation under the existing stress direction. The stress-induced transformation is important for the SMA. When the transformation is induced only by the temperature, the SMA will lose all its typical deformation behavior. And for a given SMA, its deformation behavior can change from pseudoelasticity to the shape-memory effect with the decrease of the experimental temperature. In order to model the deformation behaviors of SMA, it is necessary to incorporate correctly stress-induced transformation process and its relation with the temperature.

The relation between stress τ and transformation strain γ^t in the process of stress-induced martensite transformation and its reverse transformation is shown in Fig. 2. In Fig. 2, T means the experimental temperature; OABC, and CDEO are the loading and unloading processes, respectively; $\tau^{MS}(T)$, $\tau^{MF}(T)$, $\tau^{AS}(T)$ and $\tau^{AF}(T)$ are the martensite transformation starting, finishing stresses (critical stress) and the austenite transformation starting, finishing stresses (critical stress) under temperature T, respectively; γ^t_{MAX} is the maximum transformation strain determined by its crystallographic structure. Thereafter, the stress–strain relation in the stress-induced martensite transformation and its reverse (austenite) transformation processes can be expressed by the

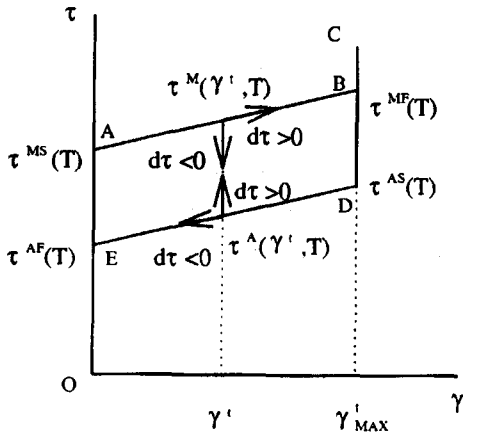

Fig. 2. Relation between the shear stress and transformation strain in the martensite variant.

following equations:

$$\tau^M(\gamma^t, T) = \tau^{MS}(T) + H\gamma^t, \quad \tau^A(\gamma^t, T) = \tau^{AF}(T) + H\gamma^t, \tag{1}$$

where H is the hardening coefficient.

Moreover, $\tau^{MS}(T)$ and $\tau^{AF}(T)$ are the temperature-dependent variables, and it is simply assumed that there is a linear relation between such critical stresses and temperature:

$$\tau^{MS}(T) = \tau_0^{MS} + \beta(T - T_0), \quad \tau^{AF}(T) = \tau_0^{AF} + \beta(T - T_0), \tag{2}$$

where β is the temperature coefficient, τ_0^{MS} and τ_0^{AF} can be seen as the transformation critical stresses under reference temperature T_0, e.g., the room temperature. Therefore, for the stress-induced martensite transformation, the deformation behavior or stress–strain relation under a given temperature T can be decided by the critical transformation stresses under reference temperature T_0: τ_0^{MS}, τ_0^{AF}, and three other constants: γ_{MAX}^t, H and β. All the other critical stresses can be obtained by the following equations:

$$\tau^{MF} = \tau^{MS}(T) + H\gamma_{MAX}^t, \quad \tau^{AS}(T) = \tau^{AF}(T) + H\gamma_{MAX}^t, \tag{3}$$

$$\tau_0^{MF} = \tau_0^{MS} + H\gamma_{MAX}^t, \qquad \tau_0^{AS} = \tau_0^{AF} + H\gamma_{MAX}^t. \tag{4}$$

So Eqn (1) can be written as follows:

$$\mathrm{d}\tau^M(\gamma^t, T) = \beta\,\mathrm{d}T + H\,\mathrm{d}\gamma^t, \mathrm{d}\tau^A(\gamma^t, T) = \beta\,\mathrm{d}T + H\,\mathrm{d}\gamma^t. \tag{5}$$

According to above thermo-mechanical model, the process of the stress-induced martensite transformation or the temperature-induced uniformly twinned deformation under the assistance of stress and its reverse transformation can be expressed by the following equations, of which $\mathrm{d}\tau$ is the increment of shear stress in the transformation system; $\mathrm{d}T$ is the increment of the temperature: $\mathrm{d}\gamma^t$ is the increment of transformation strain. In the loading ($\mathrm{d}\tau > 0$) and unloading ($\mathrm{d}\tau < 0$) processes under constant temperature ($\mathrm{d}T = 0$),

$\mathrm{d}\tau > 0$ and $\tau < \tau^M(\gamma^t, T)$: $\mathrm{d}\gamma^t = 0$,

$\mathrm{d}\tau > 0$, $\tau = \tau^M(\gamma^t, T)$ and $\gamma^t < \gamma_{MAX}^t$: $\mathrm{d}\gamma^t = \mathrm{d}\tau/H$,

$\mathrm{d}\tau > 0$ and $\gamma^t = \gamma_{MAX}^t$: $\mathrm{d}\gamma^t = 0$,

$\mathrm{d}\tau < 0$, $\tau > \tau^A(\gamma^t, T)$: $\mathrm{d}\gamma^t = 0$,

$\mathrm{d}\tau < 0$, $\tau = \tau^A(\gamma^t, T)$ and $\gamma^t > 0$: $\mathrm{d}\gamma^t = \mathrm{d}\tau/H$,

$\mathrm{d}\tau < 0$ and $\gamma^t = 0$: $\mathrm{d}\gamma^t = 0$.

In the temperature cycles under a constant stress ($d\tau = 0$),

$dT > 0$, and $\tau > \tau^A(\gamma^t, T)$: $d\gamma^t = 0$

$dT > 0$, $\tau = \tau^A(\gamma^t, T)$ and $\gamma^t > 0$: $d\gamma^t = -\dfrac{\beta}{H} dT$

$dT > 0$, and $\gamma^t = 0$: $d\gamma^t = 0$

$dT < 0$ and $\tau < \tau^M(\gamma^t, T)$: $d\gamma^t = 0$

$dT < 0$, $\tau = \tau^M(\gamma^t, T)$ and $\gamma^t < \gamma^t_{MAX}$: $d\gamma^t = -\dfrac{\beta}{H} dT$

$dT < 0$ and $\gamma^t = \gamma^t_{MAX}$: $d\gamma^t = 0$

2.2. *Crystal component model*

In the crystal model, it is assumed that the number of potentially twinned martensite variants is K, and for the kth transformation system the twinning plane unit vector is $\mathbf{n}^{(k)} = [n_1^{(k)}, n_2^{(k)}, n_3^{(k)}]$ and shear direction unit vector is $\mathbf{m}^{(k)} = [m_1^{(k)}, m_2^{(k)}, m_3^{(k)}]$. So the resolved shear stress on the kth transformation system can be calculated as follows:

$$\tau^{(k)} = \sum_{i,j=1}^{3} \alpha_{ij}^{(k)} \sigma_{ij} \quad \text{or} \quad d\tau^{(k)} = \sum_{i,j=1}^{3} \alpha_{ij}^{(k)} d\sigma_{ij}, \tag{6}$$

where $\alpha_{ij}^{(k)}$ is the generalized Schmid factor defined as follows:

$$\alpha_{ij}^{(k)} = (m_i^{(k)} n_j^{(k)} + n_i^{(k)} m_j^{(k)})/2, \tag{7}$$

and σ_{ij} is the stress tensor of a single crystal grain. That is, when the increments of stress tensor $d\sigma_{ij}$ is given, the resolved shear stress increment in the transformation system can be calculated, and then according to the phase transformation model the transformation shear strain increment $d\gamma^t_{(k)}$ can be obtained. But as a crystal model the interaction among the transformation systems, or the martensite variants, has to be considered, and a modification is necessary. That is, the transformation stress of the considered transformation system in (1) will be affected by the other transformation systems, and it is modified by using the isotropic hardening model:

$$\tau^M_{(k)}(\gamma^t_{(i)}, T) = \tau^{MS}(T) + H \sum_{i=1}^{K} \gamma^t_{(i)} \quad \text{or} \quad d\tau^M_{(k)}(\gamma^t_{(i)}, T) = \beta\, dT + H \sum_{i=1}^{K} d\gamma^t_{(i)}, \tag{8}$$

$$\tau^A_{(k)}(\gamma^t_{(i)}, T) = \tau^{AF}(T) + H \sum_{i=1}^{K} \gamma^t_{(i)} \quad \text{or} \quad d\tau^A_{(k)}(\gamma^t_{(i)}, T) = \beta\, dT + H \sum_{i=1}^{K} d\gamma^t_{(i)}. \tag{9}$$

Also it is assumed that the transformation will finish when the sum of volume fractions $\xi_{(k)}$ of the variants in the crystal is equal to 1, i.e.

$$\xi_{(1)} + \xi_{(2)} + \cdots + \xi_{(k)} + \cdots + \xi_{(K)} \leqslant 1. \tag{10}$$

For $\xi_{(k)} = \gamma_{(k)} / \gamma^t_{MAX}$, the following equation can be obtained:

$$\gamma^t_{(1)} + \gamma^t_{(2)} + \cdots + \gamma^t_{(k)} + \cdots + \gamma^t_{(K)} \leqslant \gamma^t_{MAX}. \tag{11}$$

With the calculated $d\gamma^t_{(k)}$ in this process, the transformation strain increment $d\varepsilon^t_{ij}$ of crystal grain component can be calculated as follows:

$$d\varepsilon^t_{ij} = \sum_{k=1}^{K} \alpha_{ij}^{(k)} d\gamma^t_{(k)}. \tag{12}$$

And then the total strain increment in the crystal is calculated:

$$d\varepsilon_{ij} = d\varepsilon^t_{ij} + d\varepsilon^e_{ij}, \tag{13}$$

where the $d\varepsilon^e_{ij}$ is the elastic strain increment calculated by the Hooke's law in the crystal. With such a model no matter how the crystal in the model is three-dimensional or two-dimensional, the loading

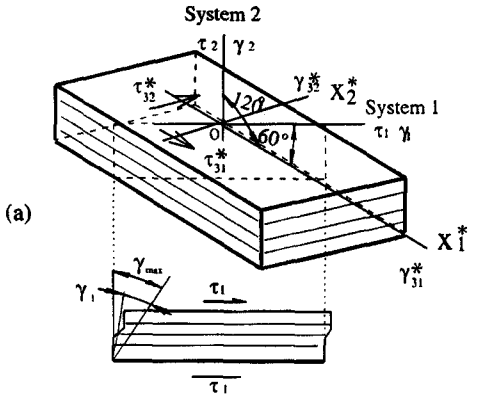

Fig. 3. Two-dimensional model of crystal grain component in the SMA.

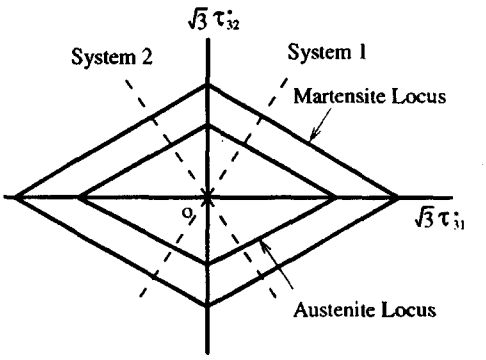

Fig. 4. Stress loci of phase transformation.

condition is complicated or is as simple as the uniaxial tension or in the temperature cycle, the deformation behavior can be calculated. For simplification, only a two-dimensional crystal model is used in the calculation, which is similar to the Tokuda's two-dimensional crystal plasticity model [9–11] when the transformation systems are considered to be analogous to the slip (or shear deformation) systems. As schematically shown in Fig. 3 it glides like a pile of play cards. But the model has some differences from the cards, i.e., this model can glide only in two directions defined by the angles which are selected as 60° and 120° measured from X_1^* axis of local coordinate system. Hereafter, these two glide systems are called twin-deformation System 1 and System 2. In the figure, τ_1 and γ_1, τ_2 and γ_2 are the shear stresses and strains of the System 1 and System 2, respectively. The τ_{31}^* and γ_{31}^*, τ_{32}^* and γ_{32}^* are the stresses and strains in the X_1^* and X_2^* directions, respectively.

The phase transformation stress loci of the two-dimensional crystal component model with two twin systems have rhombic shape as shown in Fig. 4, and they will expand with the increase of total transformation strain $\Sigma\gamma_k^t$ or the increase of the temperature T while keeping the shape similar to the original one.

2.3. *Polycrystalline model*

Here, the polycrystal is assumed to be composed of a large number of such grains with randomly distributed orientations. The interactions among grains in the model are incorporated by using the stress-constant idea, which is a special case of self-consistent scheme [12], i.e., the stress of the grain, σ_{ij}, is the same as the macroscopic stress Σ_{ij},

$$\sigma_{ij} = \Sigma_{ij}. \tag{14}$$

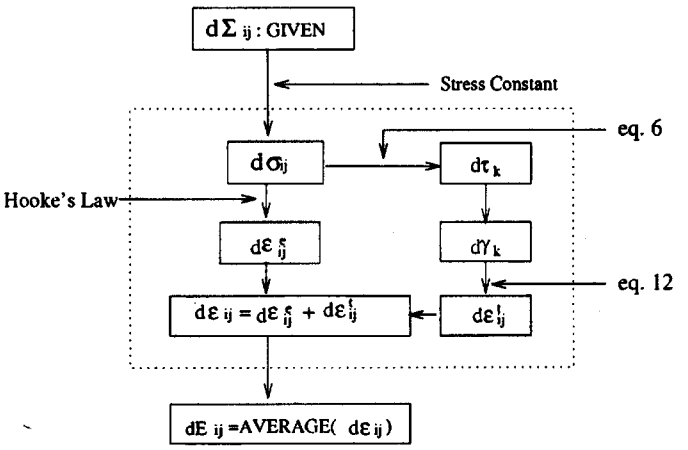

Fig. 5. Flowchart of calculation process.

The macroscopic strain E_{ij} is the average of the strains ε_{ij} of every grains:

$$E_{ij} = \text{AVERAGE}(\varepsilon_{ij}). \tag{15}$$

The above calculation process can be totally expressed by the flowchart shown in Fig. 5.

3. CALCULATION RESULTS AND COMPARISON WITH THE EXPERIMENTAL RESULTS

In the calculation the material constants are selected as follows:

$$\gamma^t_{\text{MAX}}/\sqrt{3} = 2.5\%, \quad \tau_0^{MS} = 90.0\,\text{MPa}, \quad \tau_0^{AF} = 70.0\,\text{MPa}, \quad H = 5.0 \times 10^2\,\text{MPa}.$$

$$\beta = 50.0\,\text{MPa/K}, \quad G = 16.6\,\text{GPa}$$

The stress vector $\bar{\sigma}$ is defined as $\bar{\sigma} = (\sqrt{3}\tau_{31}, \sqrt{3}\tau_{32})$ and the strain response is described as a strain vector $\bar{\gamma} = (\gamma_{31}/\sqrt{3}, \gamma_{32}/\sqrt{3})$.

The used shape memory alloy in the experiments [1–3] is a polycrystalline Cu-based alloy: Cu–10 wt% Al–5 wt% Zn–5 wt% Mn. The fundamental phase transformation temperatures of this material under no-loading are as follows:

$$T^{MS} = 239\,\text{K}, \quad T^{MF} = 223\,\text{K}, \quad T^{AS} = 248\,\text{K}, \quad T^{AF} = 260\,\text{K},$$

where T^{MS} and T^{MF} are the starting and finishing temperatures of martensite transformation, respectively; T^{AS} and T^{AF} are the starting and finishing temperatures of austenite transformation, respectively. A thin-wall tube was machined, whose outer diameter is 8 mm, inner diameter is 5 mm, gauge length is 40 mm. The apparatus is the Shimadzu-AG10TC Autograph [1–3] which can apply the complex multi-axial loading and heat up the specimen. By using the specimen and the apparatus, a series of multi-axial loading tests, some of which are with temperature changes, were performed.

In the experimental results, σ and ε are the axial stress and strain components of the thin-walled tubular specimen, respectively, τ and γ are the shear stress and strain components of the specimen, respectively. The stress vector $\bar{\sigma}$ is defined as $\bar{\sigma} = (\sigma, C_1\tau)$, and the strain response is described by a strain vector $\bar{\varepsilon} = (\varepsilon, C_2\gamma)$. The coefficients C_1 and C_2 are material constants to adjust the relation between shear stress τ and shear strain γ, which is obtained from the uniaxial torsion test, to the relation between the stress σ and strain ε, which is obtained from the uniaxial tension test [1–3].

Figure 6 shows an example of complex stress paths and the corresponding strain responses obtained by the calculation and the experiment. Figure 6(a) shows the complex stress paths. They can be in the clockwise or in the anti-clockwise, for example, along OBAO or OABO. Figure 6(b) shows the strain responses to the stress paths OBAO and OBCO, which are obtained by the calculation. Figure 6(d) shows the corresponding experimental results. Figure 6(c) shows the strain

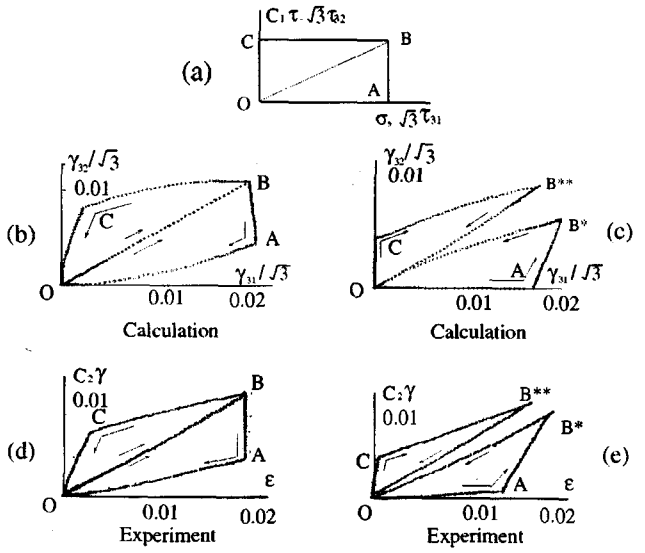

Fig. 6. Calculated and experimental results of deformation behaviors under complex loading conditions.

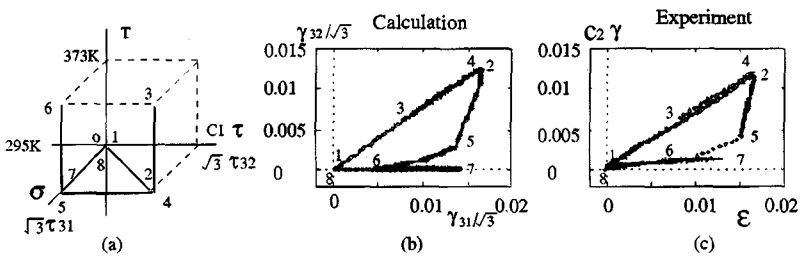

Fig. 7. Calculated result and experimental results of deformation behavior in the temperature cycles under complex loading conditions.

responses to the stress paths OCBO and OABO, which are obtained by the calculation. Figure 6(e) shows the corresponding experimental results. Comparing the calculated results and experimental results, they are very similar. Also, even along the same stress path but in the different directions OBAO and OABO in Fig. 6(a), the strain response OB**AO in Fig. 6(b) and OAB*O in Fig. 6(c) are significantly different with each other, i.e., the shape memory alloy has a path-dependent deformation behavior. The shape of strain response, as the plastic deformation, is rather different from the original shape of stress path, for example, there is a significant difference between the OBAO in Fig. 6(a) and OBAO in Fig. 6(b), but in every case the zero stress state always corresponds to the zero strain state as in the elastic deformation. The computed result reproduced very well these interesting as well as important features of SMA.

Figure 7 shows the deformation behavior of SMA in the temperature changing process under the complex loading condition. Figure 7(a) shows the loading process, in which $1 \rightarrow 2$ is the proportional loading of $\sqrt{3}\tau_{31}$ and $\sqrt{3}\tau_{32}$ in the calculation process or proportional loading of σ and $C_1\tau$ in the experiment; at point 2, the temperature is raised to point 3(373 K) from point 2(295 K) first and then decreased to point 4(295 K) while keeping the stress unchanged; the path $4 \rightarrow 5$ is the unloading process of $\sqrt{3}\tau_{32}$ in the calculation or $C_1\tau$ in the experiment; at point 5, the same temperature cycle $5 \rightarrow 6 \rightarrow 7$ (as at point 2) is applied; $7 \rightarrow 8$ is the unloading process of $\sqrt{3}\tau_{31}$ in the calculation or σ in the experiment. Figure 7(b) shows the strain response obtained by the calculation and Fig. 7(c) shows the corresponding experimental results. As the experimental results, from these calculation results it is found that under the proportional loading condition as $1 \rightarrow 2$ the original strain is recovered after the temperature cycle, i.e., the strain state of point 4 is the same as point 2. And such phenomenon can be called the shape-memory effect under loading. On the other hand, under

non-proportional multi-axial complex loading condition, the original strain cannot be recovered after the temperature cycle, i.e., the strain state of point 7 is different from the strain state of point 5. It means that the SMA will lose such memory ability in the temperature cycle after a complex loading history. The reason may be that some martensite variants produced in the previous loading history will disappear in the temperature cycle. Obviously, almost all the important phenomena found in the experiment can be obtained in the calculation.

4. CONCLUSION

In this paper we present the two-dimensional mechanical model of SMA. With the set up model, the mechanical deformation behaviors of the SMA under complex multi-axial loading process with the temperature changes can be calculated. By the calculation of the model, the experimental results, i.e., the pseudoelastic deformation behavior of the SMA, and the loss of the shape-memory effect at certain complex loading condition, are reproduced qualitatively. It can be thought that the model can be used to predict the mechanical behavior of the shape-memory alloy under the complicated loading conditions, and it will be very useful for the design of the intelligent device.

REFERENCES

1. Sittner, P., Hara, Y. and Tokuda, M., SMA hysteresis under combined tension and torsion. *Proceedings of the International Symposium on Shape Memory Alloy Materials*, Beijing. International Academic Publishers, 1994, pp. 541–545.
2. Sittner, P. and Tokuda, M., Thermoelastical Martensite transformation under combined stress—simulation and experiment. *Proceedings of the 15th Riso International Symposium on Materials Science*, Denmark, 1994, pp. 537–544.
3. Sittner, P., Hara, Y. and Tokuda, M., The stabilization of transformation pathway in stress induced Martensite. *Scripta Metallurgica et Materialia*, 1995, **32**(12), 2073.
4. Falk, F. Model free energy, mechanics, and thermodynamics of shape memory alloys. *Acta Metallurgica*, 1980, **28**, 1773.
5. Tanaka, K., Thermo-mechanical sketch of shape memory effect: one-dimensional tensile behavior. *Research Mechanics*, 1986, **18**, 251.
6. Tanaka, K., Kobayashi, S. and Sato, Y., Thermomechanics of transformation pseudoelasticity and shape memory effect in alloys. *International Journal of Plasticity*, 1986, **2**, 59.
7. Muller, I. and Xu, H., On the pseudo-elastic hysteresis. *Acta Metallurgica et Materialia*, 1991, **39**(3), 263–271.
8. Raniecki, B. and Lexcellent, C., R_L-models of pseudoelasticity and their specification for some shape memory solids. *European Journal of Mechanics, A/Solids*, 1994, **13**(1), 21.
9. Tokuda, M. and Katoh, H., Role of multi-slip on polycrystalline behaviors of polycrystalline metals. *Bulletin of the JSME*, 1986, 29–249, 708–715.
10. Tokuda, M., Havlicek, F., Sittner, P. and Kratochvil, J., Computational study on accommodation parameter in self-consistent model, *Research Reports on the Faculty of Engineering, Mie University*, 1992, **17**, 1–19.
11. Tokuda, M., Sittner, P. and Hara, Y., Constitutive equations of polycrystalline SMA. *Proceedings of the National Congress of Theoretical and Applied Mechanics*, 1994, pp. 671–672.
12. Hutchinson, J. K., Polycrystalline stress-strain relations of F.C.C. polycrystalline metals hardening according to Taylor's rule. *Journal of Mechanical Physics of Solid*, 1964, **12**, 11.